Effect of acetic acid on optical coherence tomography (OCT) images of cervical epithelium

Julia Gallwas, Anna Stanchi, Christian Dannecker, Nina Ditsch, Susanna Mueller, Uwe Mortensen, Herbert Stepp

Angaben zur Veröffentlichung / Publication details:

Gallwas, Julia, Anna Stanchi, Christian Dannecker, Nina Ditsch, Susanna Mueller, Uwe Mortensen, and Herbert Stepp. 2014. "Effect of acetic acid on optical coherence tomography (OCT) images of cervical epithelium." Lasers in Medical Science 29 (6): 1821–28. https://doi.org/10.1007/s10103-014-1581-9.

Effect of optical clearing agents on optical coherence tomography images of cervical epithelium

Julia Gallwas · Anna Stanchi · Nina Ditsch · Theresa Schwarz · Christian Dannecker · Susanna Mueller · Herbert Stepp · Uwe Mortensen

Abstract Optical coherence tomography (OCT) can be used as an adjunct to colposcopy in order to detect precancerous and cancerous cervical lesions. Optical clearing agents (OCAs) temporarily reduce the optical scattering of biological tissues. The purpose of this study was to investigate their influence on OCT imaging. OCT images were taken from unsuspicious and suspicious areas of fresh conization specimens immediately after resection and 5, 10, and 20 min after application of dimethyl sulfoxide (DMSO) or polyethylene glycol (PEG). Corresponding histologies were obtained from all sites. The images taken 5, 10, and 20 min after application of OCA were compared to the initial images with respect to changes in brightness, contrast, and scanning depth using a standard nonparametric test of differences of proportions. Further, mean intensity backscattering curves were calculated from all OCT images in the histological groups CIN2, CIN3, inflammation, and normal epithelium. Mean difference profiles within each of these groups were determined, reflecting the mean differences between the condition before the application of OCA and the exposure times 5, 10, and 20 min, respectively. The null hypothesis was tested employing the Dicky-Fuller-test, Hotelings-test and run test. The visual analysis of 434 OCT images from 109 different sites of 24 conization specimens showed a statistically significant increase in brightness and contrast for normal and dysplastic epithelium after application of DMSO or PEG. Further, the analysis of mean intensity profiles suggests the existence of an increased backscattering intensity after application of DMSO or PEG. DMSO and PEG contribute substantially to optical clearing in cervical squamous epithelium and therefore influence OCT imaging in a positive way. With further refinement of the OCT technology, the observed changes may be beneficial in interpreting the tissue microstructure and identifying cervical intraepithelial neoplasia.

Keywords Optical coherence tomography · OCT · Acetic acid · Colposcopy · Cervix uteri

J. Gallwas A. Stanchi · N. Ditsch · T. Schwarz · C. Dannecker
Department of Obstetrics and Gynecology, Ludwig Maximilians University Munich, Großhadern Medical Campus, Marchioninistr. 15, 81377 Munich, Germany
e-mail: juliagallwas@aol.com

S. Mueller
Department of Pathology, Ludwig Maximilians University Munich, Großhadern Medical Campus, Marchioninistr. 15, 81377 Munich, Germany

H. Stepp
Laser Forschungs Labor—Life Science Centre, Ludwig Maximilians University Munich, Marchioninistr. 15, 81377 Munich, Germany

U. Mortensen
Department of Psychology, Westfälische Wilhelms-University, Muenster, Germany

Introduction

Optical coherence tomography (OCT) has been shown to provide information useful in the detection of cervical intraepithelial neoplasia (CIN) [1–4]. It permits the characterization of cervical squamous epithelium up to 2 mm in depth and can be used as an adjunct to colposcopy [3–5]. OCT images of normal cervical epithelium reveal a well-organized layered architecture with a sharp interface separating epithelium and stroma. This is the result of different optical scattering coefficients for epithelium (poorer scattering) and stroma (brighter scattering) [1, 2]. The basal membrane itself is too thin to be visualized by OCT. In mild dysplasia (CIN1) the morphological changes are confined to the basal 1/3 of the epithelium. OCT images show a less clear but still intact borderline between epithelium and underlying stroma. CIN 2 and CIN 3 are characterized by increasing

irregularity and thickening of the epithelial layer while OCT images of invasive carcinoma display a complete lack of layer architecture (Fig. 1). The basement membrane is no longer intact and the epithelium becomes an unstructured homogeneous highly backscattering region. OCT images of inflammatory changes display edema of the epithelium and stromal layer [1, 3, 4, 6].

One of the limitations of OCT is that the depth of light penetration is restricted by absorption and scattering. At near-infrared wavelengths, scattering dominates over absorption and therefore is more significant in reducing the penetration of light into the tissue. The local application of hyperosmotic chemical agents such as dimethyl sulfoxide (DMSO) or polyethylene glycol (PEG) represents a well-known method for reducing light scattering and thereby enhancing the penetration of light. Various mechanisms for the optical clearing effect have been discussed such as dehydration, refractive index matching between the scatterers and the surrounding medium as well as collagen dissociation [7–12].

The purpose of this study was to investigate whether optical clearing agents (OCAs) such as DMSO or PEG substantially alter the quality of OCT images and improve the detection of dysplastic cervical lesions.

Methods

This prospective single-institution ex vivo study was approved by the Institutional Review Board of the Medical Faculty of the University of Munich.

OCT images were obtained from four to six designated sites of loop electrosurgical excision procedure (LEEP) specimens. From each site, images were generated immediately after resection and 5, 10, and 20 min after application of dimethyl sulfoxide (CryoSure-DMSO, WAK Chemie Medical GmbH) or polyethylene glycol (PEG, molecular weight 400, Aldrich Co., St. Louis, Missouri, USA). During the investigation period, the specimens were kept moist using gauze soaked in 0.9 % NaCl. Finally, biopsies were taken from all sites.

The OCT images of each group (before application, 5, 10, and 20 min after application of either DMSO or PEG) were blinded with respect to their origin and classified by an investigator not involved in the original imaging process using the following criteria: normal epithelium, cylindrical epithelium, inflammation, CIN1, CIN2, CIN3, and carcinoma. These findings were later matched to the corresponding histology.

Second, all OCT images taken after application of DMSO or PEG were compared to the initial images regarding changes in overall brightness, contrast, and scanning depth using a

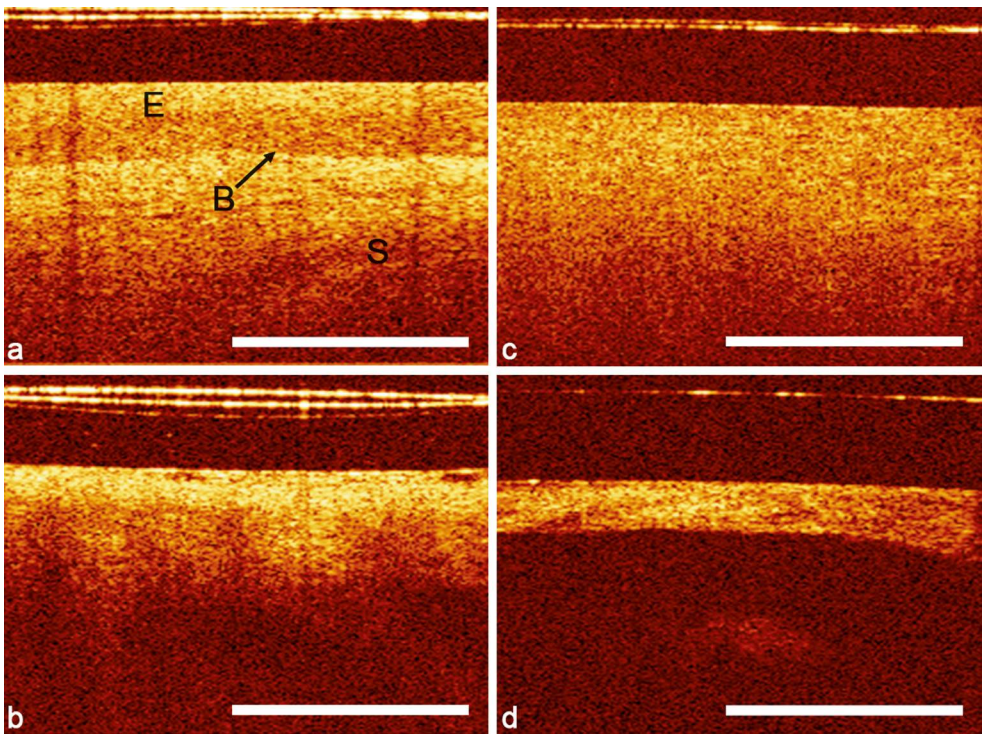

Fig. 1 **a** OCT images of normal cervical epithelium display a well-organized layered architecture with sharp borders. The thin basement membrane cannot be resolved by OCT but as it separates the epithelium from the stroma, a sharp interface can be visualized. **b** Cervical intraepithelial neoplasia grade 3 (CIN3) is characterized by a less-organized layer architecture. The stroma seems to attempt to push its way toward the surface as vertical columns. **c** Invasive carcinoma shows an unstructured homogeneous highly backscattering epithelium with a complete lack of layer architecture. The basement membrane is no longer intact or defined and the tissue microstructure is no longer organized. **d** Inflammation of the cervical epithelium is characterized by swelling and edema. The optical boundary between epithelium and underlying stroma may be more intense (*length of the white bars* 1 mm)

scale with the following ratings: 1=major decrease, 2=minor decrease, 3=no change (neutral), 4=minor increase, 5=major increase. To test the effect of the various conditions (increase/decrease), the standard test of equality of proportions was employed [13, 14] using the program prop.test from the package {stats} of the R program [15]. For reasons of sample size, the judgments of major and minor decrease had to be lumped into a category "decrease" (−); correspondingly, the minor and major increase judgments were lumped into a category "increase" (+). The no-change judgments were randomly assigned to either the decrease or the increase category, emulating a forced-choice task which avoids the notorious central tendency in judgment tasks of the type considered here. Due to this random splitting, decimal numbers instead of integers appear.

Lastly, a mean backscattering intensity profile was obtained for each OCT image by averaging all pixel values in each row and storing this mean value with its row number. Comparison or averaging of profiles was performed after manual adjustment of each profile to show the epithelial surface at the same position.

Mean backscattering intensity curves were computed by averaging over specimens of a given class and duration for all four conditions (before application and 5, 10, and 20 min after application of either DMSO or PEG). These mean profiles were considered separately for the groups "normal epithelium", "CIN2", and "CIN3" (DMSO) and "normal epithelium", "CIN3", and "inflammation" (PEG), respectively. Within each of these groups, mean difference curves (profiles) were determined, reflecting the mean differences between the condition before application of the OCA and the exposure times 5, 10, and 20 min, respectively. Furthermore, the mean differences between the exposure times 5, 10, and 20 min were computed. A mean difference profile will be called D-profile for short (D for difference) hereafter. To analyze the effect of different durations of exposure to either DMSO or PEG three statistical tests were used: (1) Hotelling's T2 test for repeated measurements was employed to test whether the mean of the differences of a D-profile differs from zero. (2) The nonparametric runs test was used to test whether there exist runs of significant length of differences of equal sign in a given D-profile; the actual sizes of the differences do not enter the test. Such runs are indicative of systematic, non-zero trends in the D-profile, and (3) the Augmented Dickey-Fuller (ADF) test was applied in order to cross-validate the results of Hotelling's test and the runs test [16].

OCT imaging was carried out using the Niris® imaging system (Imalux Corporation, Cleveland, OH), an optical fiber-based interferometer with a superluminescence diode (SLD), providing a low-coherent broadband, near-infrared light (NIR, ca. 1300 nm). The reusable fiber-optic probe with a diameter of 2.7 mm provides a depth scanning range of ≤1.5 mm and a lateral scanning range of 1.6–2.4 mm. It was used in direct contact with the tissue. The system acquires real-time images of 200×200 pixels. The Niris® imaging system has been approved by the Food and Drug Administration (FDA) and the European Community (CE).

Results

LEEP specimens were obtained from 24 women with a mean age of 32.4 years (24–47 years). All women were premenopausal, 23 women were HPV high-risk positive. The indication for conization based upon a histologically proven CIN3 in 18 cases and a persisting CIN2 in 3 cases. Three women repeatedly showed a Pap IVA on cytology. The specimens were divided into a DMSO group (n=11) and a PEG group (n=13). A total of 202 OCT images from 51 sites were evaluated in the DMSO group and 232 OCT images from 58 sites in the PEG group, respectively. Two OCT images of the DMSO group were lost in the copying process. All 434 images were compared with the corresponding histology. With respect to the different application times (0, 5, 10, 20 min), 50 (98 %), 48 (94 %), 49 (96 %), and 49 (96 %) images in the DMSO group accurately matched the histological diagnosis. In the PEG group, concordant results were obtained for 56 (97 %), 57 (98 %), 56 (97 %), and 57 (98 %) images, respectively. A beneficial effect of DMSO or PEG in interpreting the OCT images was not seen.

Ratings The assessment of OCT images regarding the influence of DMSO and PEG on brightness, contrast, and scanning depth are summarized in Figs. 2 and 3. The dichotomized data resulting from the ratings are illustrated in bar plots on the left. The tables on the right associated with each bar plot show the p value for each comparison. A significant p value indicates a significant effect of the time of exposure.

To illustrate, for the category DMSO/normal and duration B10 (brightness of normal epithelium 10 min after application of DMSO), the table provides a p value of .000 for the one-sided test indicating a statistically significant improvement. An analogous interpretation applies to the remaining data. To summarize the results for DMSO, a statistically significant increase of brightness was observed for normal epithelium, CIN2, and CIN3 independent of the duration. An increase in contrast was seen for normal epithelium and CIN3 after 10 and 20 min. An improved scanning was observed for normal epithelium after 10 and 20 min and for CIN3 independent of the exposure time. The application of PEG resulted in a statistically significant increase in brightness, contrast, and scanning depth in all three groups independent of the exposure time with the exceptions (inflammation, scanning depth, 5 min and CIN3, brightness and scanning depth, 5 min). Figure 4 gives examples of OCT images for both groups.

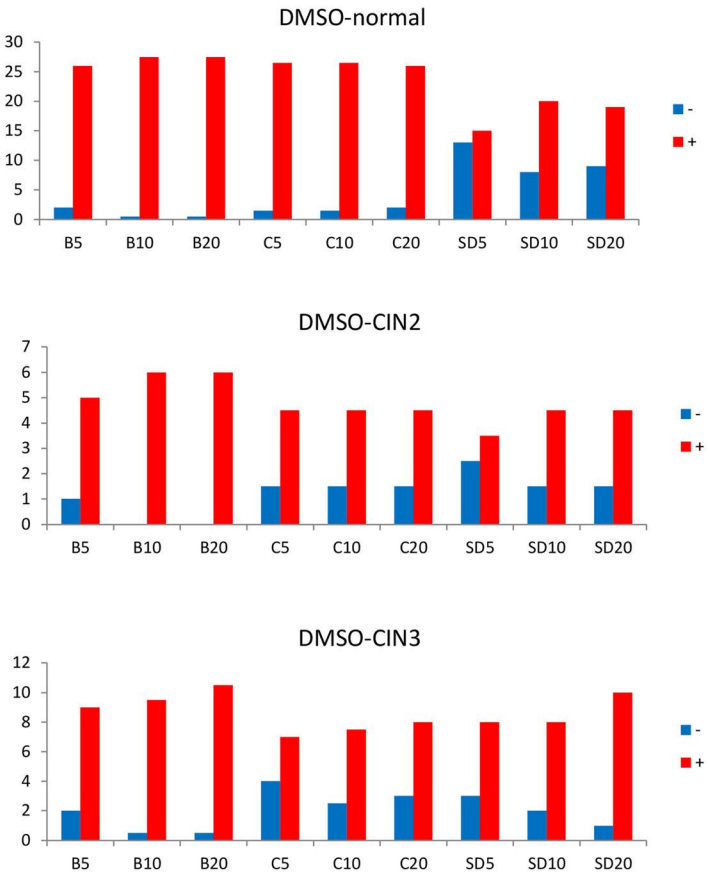

DMSO-normal		Rating						Dichotom.		
Aspect	Duration	1	2	3	4	5	∑	-	+	p
B	5	0	0	4	24	0	28	2.0	26.0	.000
	10	0	0	1	19	8	28	0.5	27.5	.000
	20	0	0	1	11	16	28	0.5	27.5	.000
C	5	0	0	3	25	0	28	1.5	26.5	.000
	10	0	1	1	18	8	28	1.5	26.5	.000
	20	0	1	2	13	12	28	2.0	26.0	.000
SD	5	0	3	20	5	0	28	13.0	15.0	.395
	10	0	3	10	13	2	28	8.0	20.0	.002
	20	0	3	12	9	4	28	9.0	19.0	.008

DMSO-CIN2		Rating						Dichotom.		
Aspect	Duration	1	2	3	4	5	∑	-	+	p
B	5	0	0	2	4	0	6	1.0	5.0	.041
	10	0	0	0	6	0	6	0.0	6.0	.002
	20	0	0	0	3	3	6	0.0	6.0	.002
C	5	0	0	3	3	0	6	1.5	4.5	.124
	10	0	1	1	3	1	6	1.5	4.5	.124
	20	0	1	1	3	1	6	1.5	4.5	.124
SD	5	0	0	5	1	0	6	2.5	3.5	.500
	10	0	1	1	4	0	6	1.5	4.5	.124
	20	0	1	1	3	1	6	1.5	4.5	.124

DMSO-CIN3		Rating						Dichotom.		
Aspect	Duration	1	2	3	4	5	∑	-	+	p
B	5	0	0	4	7	0	11	2.0	9.0	.005
	10	0	0	1	8	1	10	0.5	9.5	.000
	20	0	0	1	6	4	11	0.5	10.5	.000
C	5	0	0	8	3	0	11	4.0	7.0	.197
	10	0	0	5	5	0	10	2.5	7.5	.037
	20	0	0	6	5	0	11	3.0	8.0	.044
SD	5	0	0	6	5	0	11	3.0	8.0	.044
	10	0	0	4	6	0	10	2.0	8.0	.013
	20	0	0	2	8	1	11	1.0	10.0	.000

Fig. 2 Assessment of OCT images with respect to brightness (*B*), contrast (*C*), and scanning depth (*SD*). The dichotomized data resulting from the ratings are shown in bar plots for normal epithelium, CIN2, and CIN3 5, 10, and 20 min after application of DMSO. The corresponding tables comprehend the *p* value for each comparison, one-sided alternative

Mean intensity profiles Different exposure durations of either DMSO or PEG do have an effect on the brightness values of the specimen. However, this effect does not consist in an increase or decrease of brightness identical to all positions of a specimen. Rather, the effect consists in the formation of patterns of areas of a specimen; within these areas, brightness is either increased or decreased, and this pattern of areas depends on the particular time interval of exposure to a particular type of OCA, as well as on the correlation to a particular group (normal epithelium, inflammation, CIN2, or CIN3). With respect to a D-profile, such a pattern consists of a sequence of either increased (positive differences) or decreased (negative differences) brightness (see Figs. 5 and 6).

The sequences of either positive or negative differences in a D-profile define what may be called a trend function or simply a trend for short. The trends are induced by the type of OCA (DMSO or PEG), group, and exposure duration and appear to reflect properties of cells within the corresponding intervals.

Visual inspection of Figs. 5 and 6 shows that the trend functions in particular for the exposure time intervals of 5, 10, and 20 min are indeed rather specific for a particular OCA and a particular group. For instance, within the range of the first 20 pixels the brightness is decreased (because the differences are negative) for the condition PEG/normal epithelium, while brightness is increased (positive differences) for the condition PEG/inflammation. For the condition DMSO/normal epithelium, an increase of brightness can be observed for the first 20 pixels, while the condition DMSO/CIN2 shows a decrease of brightness which turns into an increase after 10 min. For the condition PEG/CIN3, one finds a decrease of brightness within the range of the first 10 pixels and an increase for almost all of the remaining pixels and time intervals, while in case of DMSO/CIN3 practically all trends are positive with the remarkable exception of the time interval between 5 and 10 min of exposure to DMSO.

The differences in the D-profiles appear to be small in comparison to the mean brightness values. However, the described findings are brought about by the application of Hotelling's T2-test (package \{Hotelling\} in R), which focuses on the size of the differences of a D-profile, however,

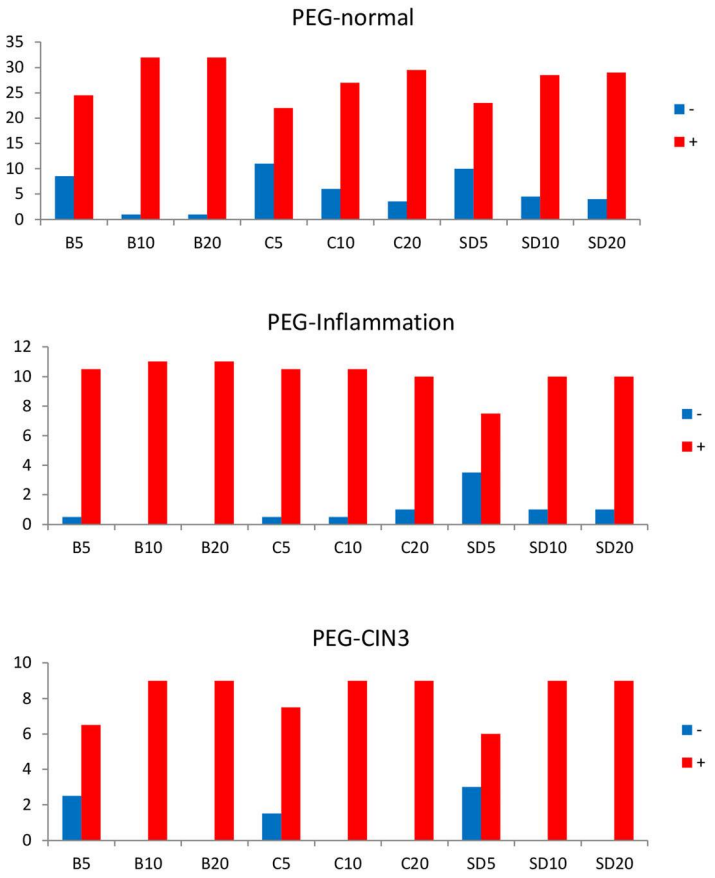

PEG-normal		Rating						Dichotom.		
Aspect	Duration	1	2	3	4	5	∑	-	+	p
B	5	0	1	15	17	0	33	8.5	24.5	.000
	10	0	0	2	21	10	33	1.0	32.0	.000
	20	0	0	2	12	19	33	1.0	32.0	.000
C	5	0	8	6	18	1	33	11.0	22.0	.007
	10	1	2	6	16	8	33	6.0	27.0	.000
	20	1	1	3	17	11	33	3.5	29.5	.000
SD	5	0	2	16	15	0	33	10.0	23.0	.002
	10	0	0	9	19	5	33	4.5	28.5	.000
	20	0	0	8	18	7	33	4.0	29.0	.000

PEG-Inflamm.		Rating						Dichotom.		
Aspect	Duration	1	2	3	4	5	∑	-	+	p
B	5	0	0	1	10	0	11	0.5	10.5	.000
	10	0	0	0	4	7	11	0.0	11.0	.000
	20	0	0	0	2	9	11	0.0	11.0	.000
C	5	0	0	1	10	0	11	0.5	10.5	.000
	10	0	0	1	8	2	11	0.5	10.5	.000
	20	0	0	2	7	2	11	1.0	10.0	.000
SD	5	0	1	5	5	0	11	3.5	7.5	.100
	10	0	0	2	9	0	11	1.0	10.0	.000
	20	0	0	2	6	3	11	1.0	10.0	.000

PEG-CIN3		Rating						Dichotom.		
Aspect	Duration	1	2	3	4	5	∑	-	+	p
B	5	0	0	5	4	0	9	2.5	6.5	.079
	10	0	0	0	8	1	9	0.0	9.0	.000
	20	0	0	0	6	3	9	0.0	9.0	.000
C	5	0	0	3	6	0	9	1.5	7.5	.009
	10	0	0	0	9	0	9	0.0	9.0	.000
	20	0	0	0	9	0	9	0.0	9.0	.000
SD	5	0	0	6	2	1	9	3.0	6.0	.173
	10	0	0	0	9	0	9	0.0	9.0	.000
	20	0	0	0	3	6	9	0.0	9.0	.000

Fig. 3 Assessment of OCT images with respect to brightness (*B*), contrast (*C*), and scanning depth (*SD*). The dichotomized data resulting from the ratings are shown in bar plots for normal epithelium, inflammation, and CIN3 5, 10, and 20 min after application of PEG. The corresponding tables comprehend the *p* value for each comparison, one-sided alternative

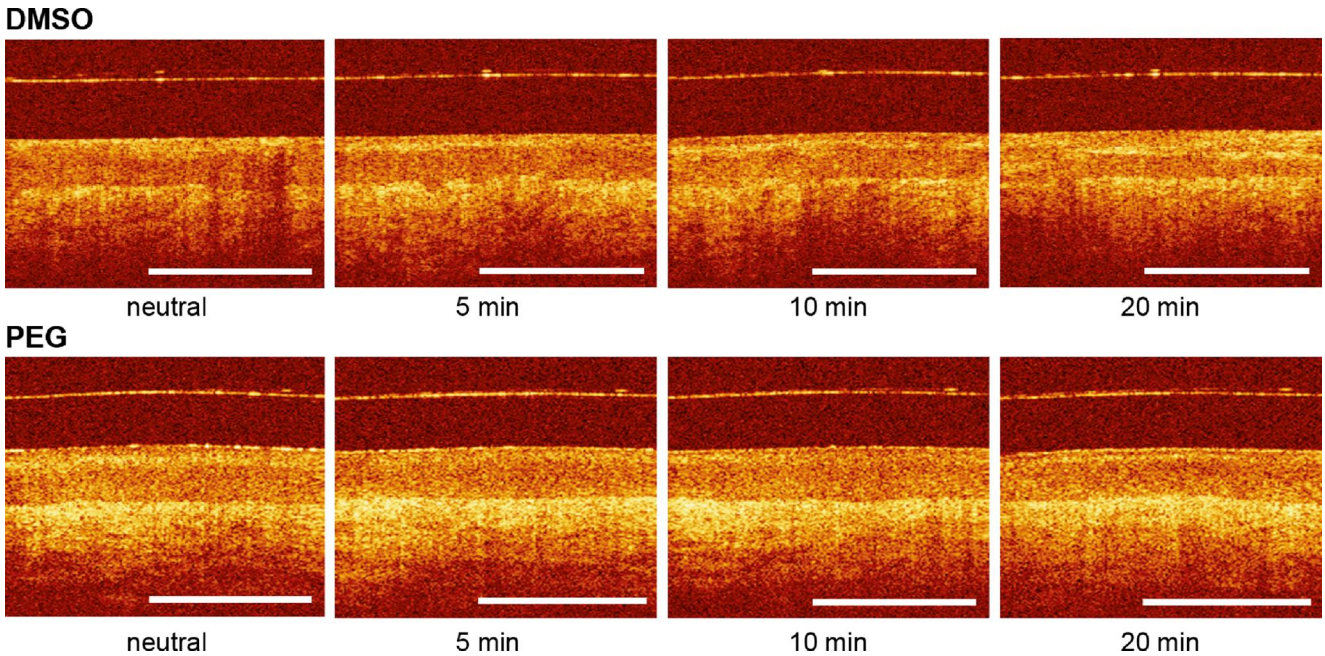

Fig. 4 OCT images of normal epithelium before (*neutral*) and 5, 10, and 20 min after application of DMSO and PEG, respectively

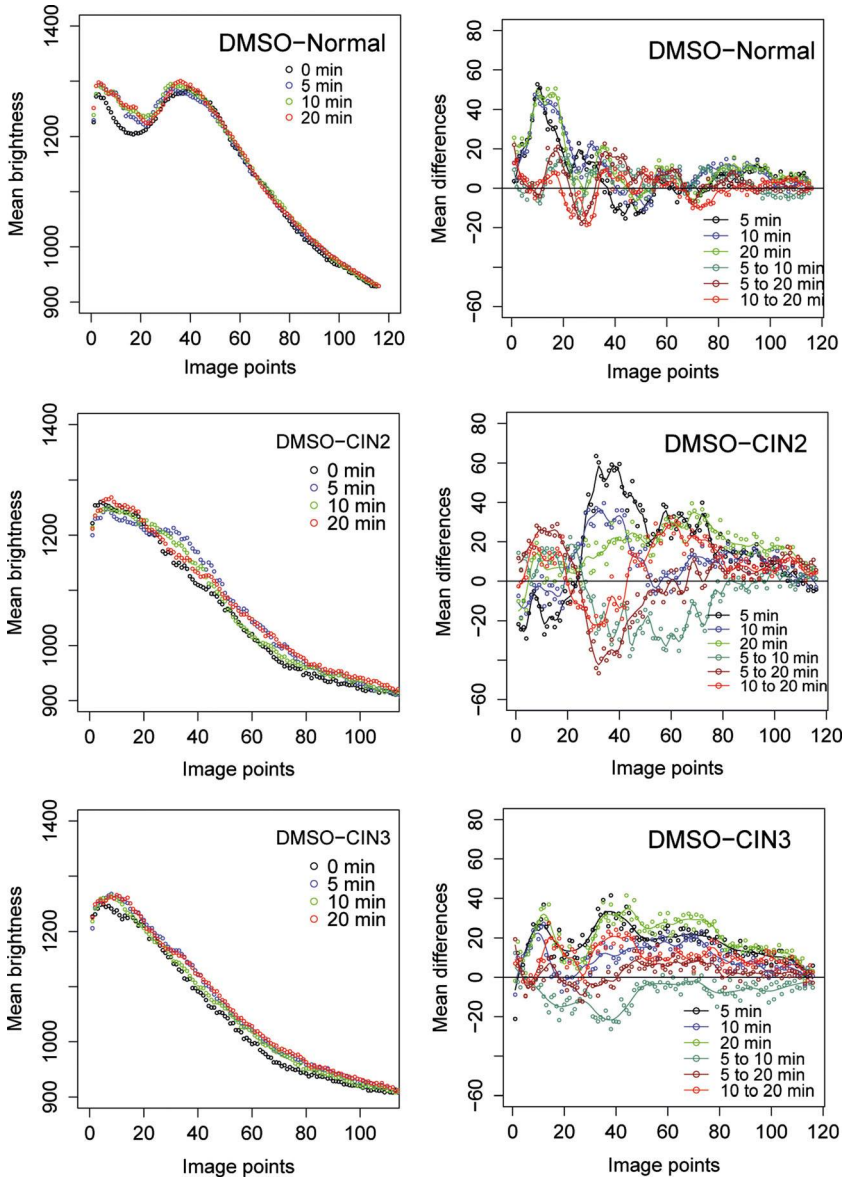

Fig. 5 Mean backscattering intensity profiles for normal epithelium, CIN2, and CIN3 before, 5, 10, and 20 min after exposure to DMSO (*left panel*). The *right panel* provides the mean difference profiles

without taking into account the patterns of sequences of either positive or negative differences (runs), and of the runs test (runs.test, package \{tseries\} in R), which focuses on the identification of such sequences (runs) without taking the sizes of the differences into account. The results of these tests were cross-validated using the ADF-test (adf.test, package \{tseries\} in R), which focuses on trends with simultaneous reference to the sizes of the differences. Since the three tests are based on different assumptions, it is remarkable that the corresponding results agree almost completely so that one has a firm basis for interpretations of the data. According to Hotelling's T2-test, the means of the differences in the D-profile differ significantly from zero ($p<.05$) except for the interval from 10 to 20 min under the condition DMSO/normal epithelium, and the first 10 min, the 20 min interval, and the interval between 10 and 20 min for the condition PEG/normal epithelium; further, the first 5 min do not seem to have any effect under the condition PEG/inflammation.

The runs test shows that each D-profile consists of sequences of either positive or negative differences of non-random lengths ($p=.000$ for all D-profiles; in order to keep Table 1 clear, these p values have not been listed) and thus supports the hypothesis that D-profiles are characterized by non-zero trend functions. For the ADF-test, the program adf.test computes p values with respect to the null hypothesis that a linear or nonlinear trend exists, so a p value greater than .05 signals the presence of a trend. According to the runs test as well as the ADF-test, all D-profiles contain a trend that reflects the non-random effect of exposure time intervals. The fact that Hotelling's T2-test does not yield significant p values for all the D-profiles may result from the fact that this test neglects the information that is contained in runs of positive or negative differences.

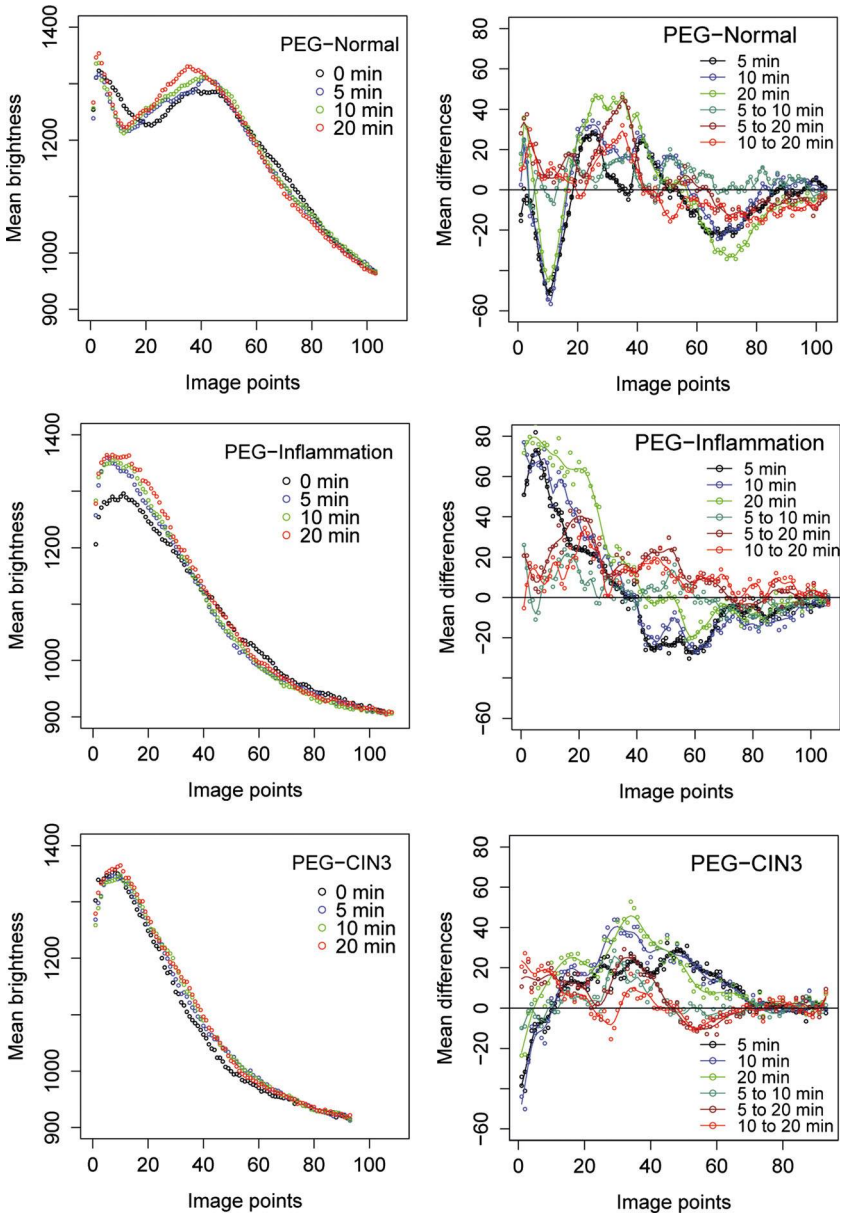

Fig. 6 Mean backscattering intensity profiles for normal epithelium, inflammation, and CIN3 before, 5, 10, and 20 min after exposure to PEG (*left panel*). The *right panel* provides the mean difference profiles

Discussion

This study shows that both DMSO and PEG have a definite effect on the absorption and scattering properties of cervical squamous epithelium. The visual changes in the OCT images regarding brightness, contrast, and scanning depth seem to be more intense for PEG as compared to DMSO, as indicated by the greater range of brightness differences under the PEG condition. These findings are consistent with other studies investigating the properties of optical clearing agents where PEG as a hydrophilic hydroxyl-terminated compound has shown to be more effective than the hydrophilic organic solvent DMSO. The modification of optical properties by optical clearing agents has been calculated from diffuse reflectance and transmission measurements in vitro and in vivo [8–11].

A central finding from the analysis of the mean profiles and the mean difference profiles is that the conditions DMSO and PEG on the one hand and in correlation to one of the groups normal epithelium, inflammation, CIN2, and CIN3 exert influences that are not independent of each other. This means that DMSO and PEG do not generate merely additive effects, regardless of the membership to one of the groups (normal epithelium, CIN2, CIN3, inflammation). Moreover, the effects of DMSO and PEG and membership to a certain group often appear to be specific to certain ranges of pixels.

The analysis of the D-profiles shows that these profiles are characterized by trends: The effect of an OCA is expressed not

Table 1 *p* values for Hotelling's *T2* (*p*(*Hot*)) and Augmented Dickey-Fuller-Test (*p*(*ADF*))

Duration (minutes)	*p* (*Hot*)	*p*(*ADF*)	*p* (*Hot*)	*p*(*ADF*)	*p* (*Hot*)	*p*(*ADF*)
	DMSO/Normal		DMSO-CIN2		DMSO-CIN3	
5	.000	.490	.000	.278	.000	.846
10	.000	.636	.000	.514	.000	.612
20	.000	.787	.000	.264	.000	.854
5 to 10	.000	.971	.000	.192	.000	.775
5 to 20	.000	.980	*.722*	.445	.000	.503
10 to 20	*.816*	.959	.000	.364	.000	.988
	PEG/Normal		PEG-Inflamm		PEG-CIN3	
5	.011	.825	*.195*	.595	.000	.691
10	*.426*	.974	.053	.961*	.000	.720
20	*.616*	.959	.000	.121	.000	.574
5 to 10	.000	.960	.004	.949	.000	.521
5 to 20	.000	.950	.000	.974	.000	.442
10 to 20	*.802*	.407	.000	.906	.007	.477

Values rendered in italics: not significant

[a] A 10-min exposure duration, condition PEG/inflammation: only a linear exists

so much in the sizes of the brightness differences but in its consistency over intervals of pixels. As the inspection of Figs. 5 and 6 shows the effect of neither DSMO nor PEG is constant over the full range of pixels. Instead, depending on the group (normal epithelium, inflammation, CIN2, CIN3) to which the tissue specimen belongs, an OCA may have a brightening ("activating") or a darkening ("inhibiting") effect on the cells within a certain range of pixels. For instance, for the first 20 to 30 pixels PEG has a darkening effect during the exposure times 5, 10, and 20 min, while for the inflammation group PEG has a brightening effect for these time intervals. On the other hand, DMSO has, for this range of pixels, a brightening effect for the durations 5, 10, and 20 min for normal epithelium, while for the inflammation group there is a darkening effect in particular during the first 5 min, while after 20 min there is a clear brightening effect. There are complex effects in the "between" intervals 5 to 10 min, 5 to 20 min, etc., and one may say that the effects of OCAs point to a complex dynamics of activating (brightening) and inhibiting (darkening) processes depending on the employed OCA, on exposure time, and on the position within a D-profile. A detailed analysis of this dynamic is beyond the scope of this paper and will require further data.

In a previous study, we investigated the influence of acetic acid on the scattering properties of cervical epithelium and could demonstrate that overall brightness and scanning depth increase with the opposite effect regarding the image contrast [17]. However, these changes had hardly any influence on the individual assessment of OCT images ex vivo as well as in vivo during OCT colposcopy. In a similar way, DMSO and PEG clearly improved the quality of the OCT images but had no clinical impact regarding the evaluation of the images. The OCT imaging was carried out with the same device we use in our colposcopy clinic. The small fiber-optic probe with a diameter of only 2.7 mm, necessary for in vivo examinations of the uterine cervix, and the acquired image resolution of 200×200 pixels certainly limit the image quality, and the clearing effect of OCA may be more distinct with more advanced OCT devices.

In contrast to acetic acid, the application of DMSO or PEG is not part of a routine colposcopic examination. Without permission from our Institutional Review Board to carry out in vivo investigations, we had to focus on an ex vivo model. In a previous study, we could demonstrate that OCT images of cervical tissue do not alter their characteristics within the first 4 h post excision [18]. Hiller et al. supported these results by validating an ex vivo human cervical tissue model for local delivery studies using biopsies from hysterectomy specimens [19]. By investigating the in vitro permeation of various molecular weight markers over a period of 24 h, no differences of permeability were observed. Therefore, we are convinced that the present results are comparable to those that would have been obtained in an in vivo setting.

This study has several biases. Although blinded to the histology results, the investigators were aware that the indication for conization was based upon a histologically proven CIN3 in most cases. Further, the investigators were familiar with the current literature and the potential optical clearing effect of DMSO and PEG. However, despite these limitations, the results are conclusive and comparable to other investigations. The optical impression of an increase in brightness was substantiated by the analysis of backscattering intensity profiles.

Over the last decade, numerous studies have reported on mechanisms and techniques for optical clearing. There prevails the strong conviction that OCAs influence optical imaging in a positive way by enhancing contrast, scanning depth, and backscattering intensity. Accordingly, this positive influence should be expected for OCT imaging as well. Despite the demonstrated effects of optical clearing agents ex vivo, it seems to be premature to assume that their application will have a clinical impact on OCT imaging at present. However, further refinement of this technology with improvements in both axial and lateral resolution together with the development of new light sources and optics may considerably increase the importance of OCA in interpreting the tissue microstructure and identifying precancerous and cancerous cervical lesions.

Acknowledgments This study was supported by grants of the Friedrich-Baur-Stiftung and Mr. and Mrs. Armin Siegl.

References

1. Turchin IV, Sergeeva EA, Dolin LS, Kamensky VA, Shakhova NM, Richards-Kortum R (2005) Novel algorithm of processing optical coherence tomography images for differentiation of biological tissue pathologies. J Biomed Opt 10, 064024
2. Bazant-Hegemark F, Edey K, Swingler GR, Read MD, Stone N (2008) Review: optical micrometer resolution scanning for non-invasive grading of precancer in the human uterine cervix. Technol Cancer Res Treat 7(6):483–496, Review
3. Escobar PF, Rojas-Espaillat L, Tisci S, Enerson C, Brainard J, Smith J, Tresser NJ, Feldchtein FI, Rojas LB, Belinson JL (2006) Optical coherence tomography as a diagnostic aid to visual inspection and colposcopy for preinvasive and invasive cancer of the uterine cervix. Int J Gynecol Cancer 16:1815–1822
4. Gallwas JMD, Turk L, Friese K, Dannecker C (2010) Optical coherence tomography (OCT) as a non invasive imaging technique for preinvasive and invasive neoplasia of the uterine cervix. Ultrasound Obstet Gynecol 36(5):624–629
5. Kang W, Qi X, Tresser NJ, Kareta M, Belinson JL, Rollins AM (2011) Diagnostic efficacy of computer extracted image features in optical coherence tomography of the precancerous cervix. Med Phys 38(1):107–113
6. Gallwas J, Turk L, Stepp H, Mueller S, Ochsenkuehn R, Friese K, Dannecker C (2011) Optical coherence tomography for the diagnosis of cervical intraepithelial neoplasia. Lasers Surg Med 43(3):206–212
7. He Y, Wang RK (2004) Dynamic optical clearing effect of tissue impregnated with hyperosmotic agents and studied with optical coherence tomography. J Biomed Opt 9(1):200–206
8. Rylander CG, Stumpp OF, Milner TE, Kemp NJ, Mendenhall JM, Diller KR, Welch AJ (2006) Dehydration mechanism of optical clearing in tissue. J Biomed Opt 11(4), 041117
9. Millon SR, Roldan-Perez KM, Riching KM, Palmer GM, Ramanujam N (2006) Effect of optical clearing agents on the in vivo optical properties of squamous epithelial tissue. Lasers Surg Med 38(10):920–927
10. Zhu Z, Wu G, Wei H, Yang H, He Y, Xie S, Zhao Q, Guo X (2012) Investigation of the permeability and optical clearing ability of different analytes in human normal and cancerous breast tissues by spectral domain OCT. J Biophotonics 5(7):536–543
11. Zhu D, Larin KV, Luo Q, Tuchin VV (2013) Recent progress in tissue optical clearing. Laser Photonics Rev 7(5):732–757
12. Genina EA, Bashkatov AN, Kolesnikova EA, Basko MV, Terentyuk GS, Tuchin VV (2014) Optical coherence tomography monitoring of enhanced skin optical clearing in rats in vivo. J Biomed Opt 19(2):21109
13. Fleiss JL, Levin B, Paik MC (2003) Statistical methods for rates and proportions, 3rd edn. Wiley, New York
14. Trapletti A, Hornik K, LeBaron B (2013) Package 'tseries' http://www.R-project.org/
15. R core Team (2003) R: a language and environment for statistical computing. R Foundation for Statistical Computing, Vienna, URL http://www.R-project.org/
16. Said E, David A (1984) Dickey: testing for unit roots in autoregressive moving average models of unknown order. Biometrika 71:599–607
17. Gallwas J, Stanchi A, Dannecker C, Ditsch N, Mueller S, Mortensen U, Stepp H (2014) Effect of acetic acid on optical coherence tomography (OCT) images of cervical epithelium. Lasers Med Sci 2014 May 15
18. Gallwas J, Mortensen U, Gaschler R, Ochsenkuehn R, Stepp H, Friese K, Dannecker C (2012) Validation of an ex vivo human cervical tissue model for optical imaging studies. Lasers Surg Med 44(3):245–248
19. Hiller C, Bock U, Balser S, Haltner-Ukomadu E, Dahm M (2008) Establishment and validation of an ex vivo human cervical tissue model for local delivery studies. Eur J Pharm Biopharm 68(2):390–399